
ADAS214: Escape Factors for Line Emission and Population Calculations

ADAS214 calculates escape factors for spectral line emission along a given line-of-sight, Θ_L , and for collisional radiative population calculations of excited levels in atoms and ions, Θ_p , on the basis of some simplifying approximations. A wide choice of spectral line profiles, spatial emission profiles and plasma geometry cases are available in the code. Doppler, Lorentz or Holtsmark profiles can be used, as well as convolutions and superpositions of different types and widths, in order to account for various line broadening mechanisms and particle groups with different temperatures. The spatial emission profiles of radiation are approximated by a polynomial fit and the code can be run for constant emission, a linear or a parabolic decrease from the plasma centre to the edge. The population escape factor can be calculated in the centre of a plasma sphere, in the mid-plane of a disk, or on the axis of a cylinder. The underlying definitions of the present escape factor analysis and the approximations in the solution of the equation of radiative transfer are explained in the background theory below. Normalised escape factors for Θ_L , and Θ_p for the described cases are shown and the consequences of the different models are discussed. An example of the use of the code is also given, with emphasis on the choice of input parameters. In the past, the described program had already been applied to many other studies of opacity including the calculation of ionisation, recombination and radiation coefficients on the basis of the ADAS atomic data base. Much of the information in this section is taken directly from the report of Behringer [10] which describes the visual basic program that ADAS214 is based on.

Background theory:

The optical thickness of resonance lines plays an important role in many laboratory and astrophysical plasmas, e.g. low-density, low-temperature discharges for plasma technology. However, radiative transfer in hydrogen resonance lines has also become an important issue in present-day divertor plasmas, as e.g. realised in ASDEX Upgrade, due to strong net volume recombination resulting in high neutral densities. This opacity affects the emitted radiance of spectral lines, but also changes the population of excited states and the effective collisional-radiative ionisation and recombination rate coefficients. In order to deal with the consequences of radiative transfer, the escape factor method has been widely used both in astrophysics and plasma physics (see e.g. Irons [1] for an overview). In the following report, a relatively simple evaluation and application of escape factors will be discussed for both interpreting optically thick line emission and for dealing with the change in excited state populations due to re-absorption of radiation. The basic model described here was implemented in a PC computer code quite some time ago by Behringer and applied to the study of an air-like plasma jet [2, 3]. The code has been amended and extended since, and a later version has been used for analysing opacity problems in low temperature divertor plasmas [4]. Various models for plasma geometry and spectral line profiles have been made available in the course of time. The numerical program was originally written in BASIC for DOS, and was later translated to Visual Basic for WINDOWS 95. ADAS214 contains a direct translation of this code together with all the processing options of the previous PC code. It also includes evaluation of the escape factor modified populations and emission as the absorber density (or plasma dimension) is scanned, for reviewing sensitive line ratios.

Basic Equations and Simplifying Approximations

Definition of Escape Factors:

The spectral radiance $L_\lambda(\lambda)$ in a plasma along a line of sight l is given by the equation of radiative transfer (without scattering into the line-of-sight):

$$\frac{dL_\lambda}{dl} = \varepsilon_\lambda - \alpha' L_\lambda \quad 3.14.1$$

where ε_λ is the spectral emission coefficient and α' is the effective absorption coefficient, which is obtained by subtracting stimulated emission from direct absorption (absorption coefficient α). If the population ratio of upper and lower states can be described by a Boltzmann distribution according to the temperature T , α' is given by $\alpha[1 - \exp(-h\nu/kT)]$. For most applications, the stimulated emission correction is small and in practice may be even smaller due to under-population of the excited states. Therefore, stimulated emission will be neglected in the following discussion, i.e. α' will be replaced by α . The spectral emission coefficient within a spectral line can be derived from the line emission coefficient ε_L and the spectral line profile $P_\lambda(\Delta\lambda)$, which must be calculated on the basis of the relevant line broadening mechanisms in the plasma:

$$\varepsilon_\lambda(\lambda) = \varepsilon_L P_\lambda(\Delta\lambda), \quad \varepsilon_\lambda(\lambda) = \frac{n_k A_{k \rightarrow j} h\nu}{4\pi} P_\lambda(\Delta\lambda) \quad 3.14.2$$

In equation 3.14.2, n_k is the number density in the upper state k and $A_{k \rightarrow j}$ the transition probability to state j . $\Delta\lambda$ is the wavelength displacement from the line centre. If the plasma extends over the spatial co-ordinate from 0 to b , the escaping radiance at b is

$$L_\lambda(b) = \int_0^b \varepsilon_\lambda(l) \exp\left[-\int_l^b \alpha(l') dl'\right] dl + L_\lambda(0) \exp\left[-\int_0^b \alpha(l) dl\right] \quad 3.14.3$$

In the following, the assumption will be made that α is independent of l and equal to $\bar{\alpha}$. In essence this means that the absorber density is constant in the plasma, which is true for neutrals in low density plasmas and probably a good first approximation to the conditions for neutrals in detached divertor plasmas, and many astrophysical plasmas. Still, it is probably the most restricting condition of the present escape factor discussion. Equation 3.14.3 then becomes, with $L(0) = 0$:

$$L_\lambda(b) = \int_0^b \varepsilon_\lambda(l) \exp[(l-b)\bar{\alpha}] dl \quad 3.14.4$$

As a further simplification, we adopt a spatially constant line profile P_λ for both emission and absorption. Again, this limitation should not be too severe for cold fusion divertor plasmas and astrophysical plasmas, where P_λ , is determined by the thermal motion of neutral particles acquired from Franck Condon energy or from charge exchange reactions, and where the mean-free path of these particle is long compared to the plasma dimensions. In principle, the presented code could be restructured to take into account the spatial variation of the spectral line profiles. The absorption coefficient is then given by the Ladenburg relation

$$\alpha(\Delta\lambda) = \alpha_t P_\lambda(\Delta\lambda), \quad \alpha(\Delta\lambda) = n_j \frac{g_k}{g_j} \frac{\lambda^4}{c} \frac{A_{k \rightarrow j}}{8\pi} P(\Delta\lambda) \quad 3.14.5$$

with statistical weights g and the Einstein coefficient $A_{k \rightarrow j}$. α_t is the wavelength-integrated absorption coefficient (nm/cm). The absorption coefficient in the line centre $\alpha(0)$ is equal to $\alpha_t P_\lambda(0)$. The escape factor for the integral line emission in the direction of l can now be defined by relating the spectral integral over the self-absorbed line profile to the optically thin line radiance. Later, b will be defined as the distance from the plasma edge to the plasma centre, therefore the line-of-sight integral must extend over $2b$:

$$\Theta_L = \frac{\int_0^{2b} \int \varepsilon_\lambda(l, \lambda) \exp[(l-2b)\bar{\alpha}(\lambda)] d\lambda dl}{\int_0^{2b} \varepsilon_L(l) dl}$$

$$\text{viz. } \Theta_L = \frac{\int_0^{2b} \varepsilon_L(l) \int_{\text{line}} P(\Delta\lambda) \exp[(l-2b)\bar{\alpha}_t P_\lambda(\Delta\lambda)] d\Delta\lambda dl}{\int_0^{2b} \varepsilon_L(l) dl} \quad 3.14.6$$

The line escape factor Θ_L in Eq. 3.14.6 describes the emitted radiance along a given line-of-sight, as required for spectroscopic measurements. It only depends on the spatial profiles over this one co-ordinate and not on the rest of the plasma geometry. For obtaining the total escaping flux, (another common definition of Θ), Eq. 3.14.6 must be integrated over solid angle and this requires more information on the plasma shape.

In order to calculate the change in excited state population due to absorption of radiation, absorption is treated as negative emission and the absorption rate is taken into account by subtracting it from the spontaneous emission rate, i.e. by reducing the transition probability in collisional-radiative model calculations. An effective reduced A-value, $A_{\text{eff}} = \Theta_p A$ is introduced, where Θ_p is determined by the relative difference between the emitted and the absorbed photon numbers (or line radiation powers) E and G :

$$\Theta_p = \frac{E - G}{E} = 1 - \frac{G}{E} \quad 3.14.7$$

The number of absorption processes in the plasma per unit volume and time, G , must be evaluated from the spectral radiance, $L_\lambda(\lambda)$, at the relevant plasma location, x , times the effective absorption coefficient, $\alpha'(x, \lambda)$, - again replaced by $\alpha(x, \lambda)$ -, integrated over wavelength and solid angle Ω . For the emitted power, the double integration simply yields 4π times the line emission coefficient $\varepsilon_L(x)$. The spectral radiance usually depends on the individual directions in the plasma, as characterised by the solid angle element $d\Omega$:

$$\Theta_p = 1 - \frac{\int \int \alpha(x, \lambda) L_\lambda(x, \lambda, \Omega) d\lambda d\Omega}{4\pi \varepsilon_L(x)} \quad 3.14.8$$

We restrict this calculation to the plasma centre or the plasma axis and adopt a point or line symmetry for the plasma parameters. If the population is evaluated for position $l = b$ in the centre of the plasma and $l = 0$ at the plasma edge where $L_\lambda = 0$, Eq. 3.14.4 can be used again:

$$\Theta_p = 1 - \frac{\int \int \alpha(b, \lambda) \int_0^b \varepsilon_\lambda(l, \lambda) \exp[(l-b)\bar{\alpha}(l, \lambda)] dl(\Omega) d\lambda d\Omega}{4\pi \varepsilon_L(b)} \quad 3.14.9$$

Since α was set constant, $\alpha(b, \lambda)$ is equal to $\bar{\alpha}(\lambda)$. For a given line profile, both Θ_L and Θ_p only depend on the product of the absorption coefficient in the line centre $\bar{\alpha}(0)$ and the length b (this product is known as the optical depth), which can be shown as follows: They represent integrals over P_λ times functions of $(\alpha_t P_\lambda b)$. The normalised profiles with width w can be written as functions of w and the wavelength distance to the line centre $\Delta\lambda$:

$$P(\Delta\lambda, w) = \frac{1}{w} V\left(\frac{\Delta\lambda}{w}\right) \quad 3.14.10$$

Introducing: $z = \frac{\Delta\lambda}{w}$

$$\int_{-\infty}^{\infty} P(\Delta\lambda) f(\alpha_t P(\Delta\lambda) b) d\Delta\lambda = \int_{-\infty}^{\infty} V(z) f\left(\frac{\alpha_t b}{w} V(z)\right) dz \quad 3.14.11$$

which means that the integrals only depend on $\frac{\alpha_l b}{w}$, i.e. on $\bar{\alpha}(0)b$. In the code, the calculations are carried out for a specific example, namely, for a wavelength $\lambda = 100nm$, for an absorption oscillator strength of 1.0, and for a Doppler width according to the input gas temperature and the element mass $w_D = 7.7$ pm for hydrogen with mass number 1.0 and 1.0eV temperature. This was originally intended for a check of the absolute results after each step, however, the calculations can clearly be re-normalised to $\bar{\alpha}(0)b$ later in the program and the parameters above just define the range of optical thickness, together with the neutral densities of the density loop. Thus the functions $\Theta_L(\bar{\alpha}(0)b)$ and $\Theta_P(\bar{\alpha}(0)b)$ need not be recalculated each time, but can be tabulated for the various cases required. In applying the escape factors to the modification of transition probabilities in ADAS *adf04* data sets, the program uses the re-normalisable tabulations and carries out a quadratic, logarithmic interpolation on the basis of the actual wavelengths, profiles and A-values in the *adf04* files (see description below).

Intensity Profiles and Plasma Geometry

The spectral radiance in the relations for both Θ_L , and Θ_P has been worked out by a polynomial fit to the spatial profile of the emission coefficient and by integrating Eq. 3.14.4 by parts:

$$L_\lambda(b) = \int_0^b \epsilon_\lambda(l) \exp[\bar{\alpha}(l-b)] dl = \frac{\epsilon_\lambda(b)}{\bar{\alpha}} - \frac{\epsilon'_\lambda(b)}{\bar{\alpha}^2} + \frac{\epsilon''_\lambda(b)}{\bar{\alpha}^3} - \dots - \exp(-\bar{\alpha}b) \left(\frac{\epsilon_\lambda(0)}{\bar{\alpha}} - \frac{\epsilon'_\lambda(0)}{\bar{\alpha}^2} + \frac{\epsilon''_\lambda(0)}{\bar{\alpha}^3} \right) - \dots, \quad 3.14.12$$

where ϵ'_λ means the first derivative with respect to l etc.

Three spatial intensity profiles have been investigated, i.e. (e1) constant emission over l , (e2) a linear increase from the edge to the plasma centre and (e3) a parabolic shape with the maximum in the centre of the plasma. The result for the integration over l is as follows:

case	integration from 0 to b (centre); $L_\lambda(b)$	integration from 0 to $2b$ (edge); $L_\lambda(2b)$
e1	$\frac{\epsilon_\lambda}{\bar{\alpha}} [1 - \exp(-\bar{\alpha}b)]$	$\frac{\epsilon_\lambda}{\bar{\alpha}} [1 - \exp(-\bar{\alpha}2b)]$
e2	$\frac{\epsilon_\lambda(b)}{\bar{\alpha}} \left(1 - \frac{1}{\bar{\alpha}b} + \frac{1}{\bar{\alpha}b} \exp(-\bar{\alpha}b) \right)$	$\frac{\epsilon_\lambda(b)}{\bar{\alpha}} \frac{1}{\bar{\alpha}b} (1 - 2 \exp(-\bar{\alpha}b) + \exp(-2\bar{\alpha}b))$
e3	$\frac{\epsilon_\lambda(b)}{\bar{\alpha}} \left[1 - \frac{2}{\bar{\alpha}^2 b^2} + \left(\frac{2}{\bar{\alpha}b} + \frac{2}{\bar{\alpha}^2 b^2} \right) \exp(-\bar{\alpha}b) \right]$	$\frac{\epsilon_\lambda(b)}{\bar{\alpha}} \frac{1}{\bar{\alpha}b} \left[2 - \frac{2}{\bar{\alpha}b} + \left(2 + \frac{2}{\bar{\alpha}b} \right) \exp(-2\bar{\alpha}b) \right]$

Table 1: Optically thick spectral radiance's for (e1) spatially constant emission, (e2) linear increase from the edge to the centre and (e3) parabolic emission profile

In the cases (e2) and (e3), $\epsilon_\lambda(b)$ is the value in the plasma centre, $\epsilon_\lambda(0) = \epsilon_\lambda(2b) = 0$. The optically thin line spectral radiances for a line-of-sight from 0 to $2b$ and for the three spatial profiles are $2b\epsilon_\lambda$, $b\epsilon_\lambda$ and $\frac{4}{3}b\epsilon_\lambda$ respectively, and the same factors apply, of course, to the wavelength-integrated radiances. If α approaches zero (almost optically thin),

the exponential functions in the above relations must eventually be expanded to avoid numerical overflow. Using the above results, the line escape factor for case (el) is e.g.:

$$\begin{aligned}\Theta_L &= \int_{line} \frac{P_\lambda}{2\bar{\alpha}(\lambda)b} [1 - \exp(-2\bar{\alpha}(\lambda)b)] d\lambda & 3.14.13 \\ &= 1 - \int_{line} P_\lambda \bar{\alpha}(\lambda)b d\lambda + \int_{line} \frac{2}{3} P_\lambda \bar{\alpha}^2(\lambda)b^2 d\lambda - \dots,\end{aligned}$$

and the population escape factor for isotropic radiation becomes

$$\begin{aligned}\Theta_P &= 1 - \frac{\int_{line} \epsilon_\lambda (1 - \exp(-\bar{\alpha}^2 b)) d\lambda}{\epsilon_L} = \int_{line} P_\lambda \exp(-\bar{\alpha}b) d\lambda & 3.14.14 \\ &= 1 - \int_{line} P_\lambda \bar{\alpha}(\lambda)b d\lambda + \int_{line} \frac{1}{2} P_\lambda \bar{\alpha}^2(\lambda)b^2 d\lambda - \dots\end{aligned}$$

Spectral Line Profiles

The following spectral line profiles have been included in the calculations: (p1) simple Doppler profiles, (p2) Lorentz profiles and (p3) Holtsmark profiles. They are given in Table 2 as a function of their full half-widths w . In addition, convolutions of Doppler and Lorentz profiles (Voigt profiles) and convolutions of Doppler and Holtsmark profiles have been provided in the program. Two superimposed Doppler profiles with different widths can be used to account for thermal or Franck-Condon and charge-exchange contributions to the emission.

case	spectral line profile (nm ⁻¹)	parameters	integration limit
p1	$P_{\lambda,D}(\Delta\lambda) = \frac{1}{1.06446w_D} \exp\left[-\left(\frac{\Delta\lambda}{0.60056w_D}\right)^2\right]$	w_D (nm)	$2.1 w_D$
p2	9	w_L (nm)	$100 w_L$
p3	$P_{\lambda,H}(\Delta\lambda) = \frac{1}{2.64261w_H} \frac{1}{1 + \left(\frac{2\Delta\lambda}{w_H}\right)^{2.5}}$	w_H (nm)	$50 w_H$
p4	Voigt profile	w_D, w_L	$200 w_L$
p5	Convolution of Doppler and Holtsmark profiles	w_D, w_H	$80 w_H$
p6	Sum of two Doppler profiles	$w_{D,1}, w_{D,2}$ $P_{D,2}(0)/P_{D,1}(0)$	$3 w_{D,2}$

Table 2: Options for spectral line profiles in the escape factor program, required input parameters and recommended spectral integration limits.

As an example, Fig. 1 shows a Doppler and a Lorentz profile, as well as their resulting Voigt profile on a semi-logarithmic scale. The Doppler width corresponds to a temperature of 1 eV, a wavelength of 100 nm and the deuterium mass. The width of the Lorentzian is one fifth of w_D . All profiles are normalised to area one. The integration over wavelength in the course of escape factor calculations are carried out numerically, which means that arbitrary spectral profiles can be used, even as tabulated values. It is also possible to deal with overlapping lines.

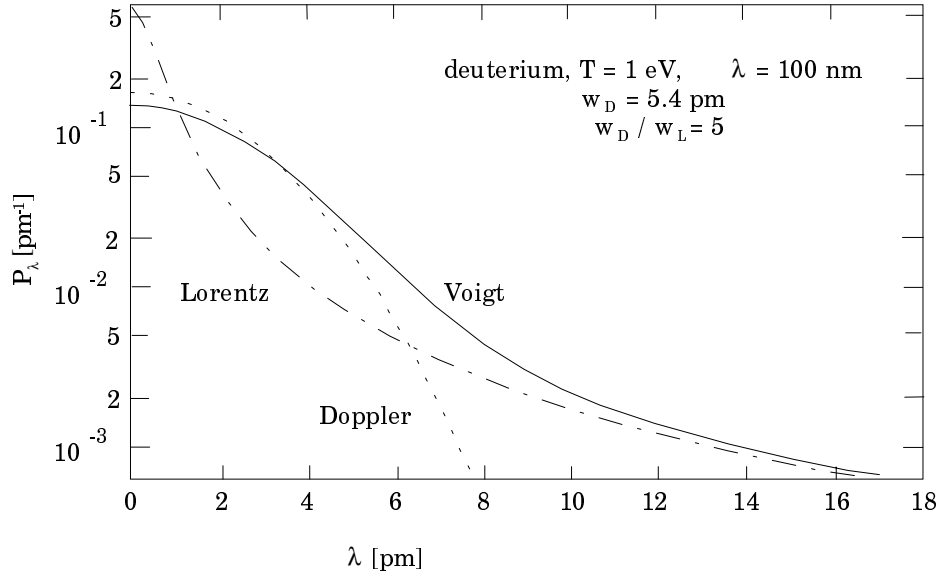


Fig. 1: Examples of Doppler and Lorentz profiles, as used in the escape factor code, and their convolution to a Voigt profile.

In code operation it is to be noted that for the profiles involving convolutions, the Doppler width is calculated from the gas temperature and atomic mass number. For the other width, it is taken as being a factor times the Doppler width, with the factor entered by the user.

According to Eq. 3.14.6, the line profiles can now be calculated for various optical thickness'. Figures 2 and 3 demonstrate the effect of self-absorption for the spatial emission cases (e1) and (e3), i.e. constant and parabolic form of the emission coefficient. In (e1) the source function $\epsilon_\lambda / \bar{\alpha}$ is constant and therefore, the spectral line shape becomes flat in the centre, while self-reversal is found in case (e3) and also in case (e2) due to a decrease in source function height between the centre and the edge of the plasma. The depression of the line centre, e.g. for (e1) and $\bar{\alpha}(0)b = 1$, can be easily calculated from Table 1 to be $\frac{1}{2}(1 - e^{-2}) = 0.4323$.

Asymptotically, $\epsilon_\lambda(0)$ falls with $\frac{1}{\bar{\alpha}(0)b}$ in case (e1) and with $\frac{1}{\bar{\alpha}(0)^2 b^2}$ in cases (e2) and (e3).

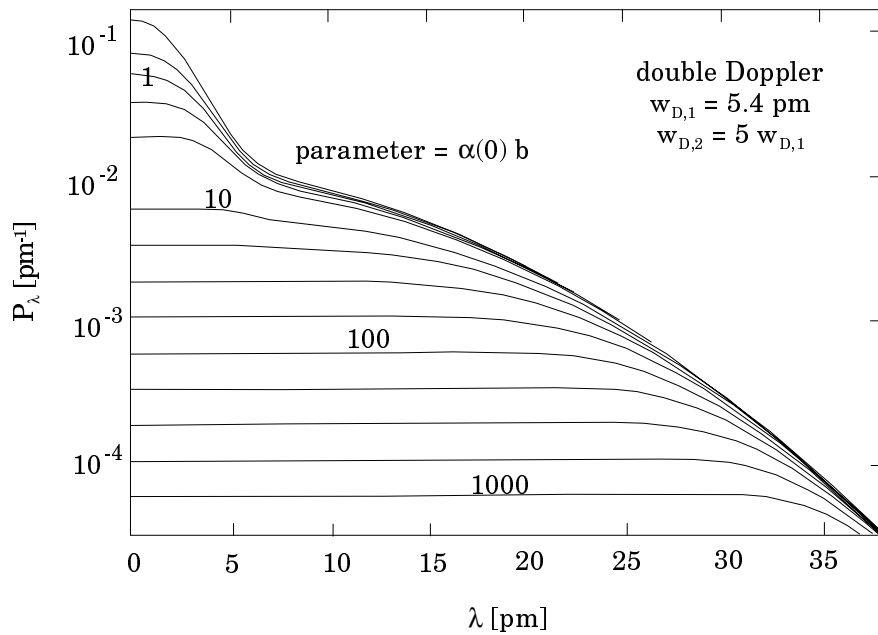


Fig. 2: Example for the calculation of spectral line profiles with various values of optical thickness. Shown is the superposition of two Doppler profiles for an emission coefficient, which is independent of plasma radius (case e1).

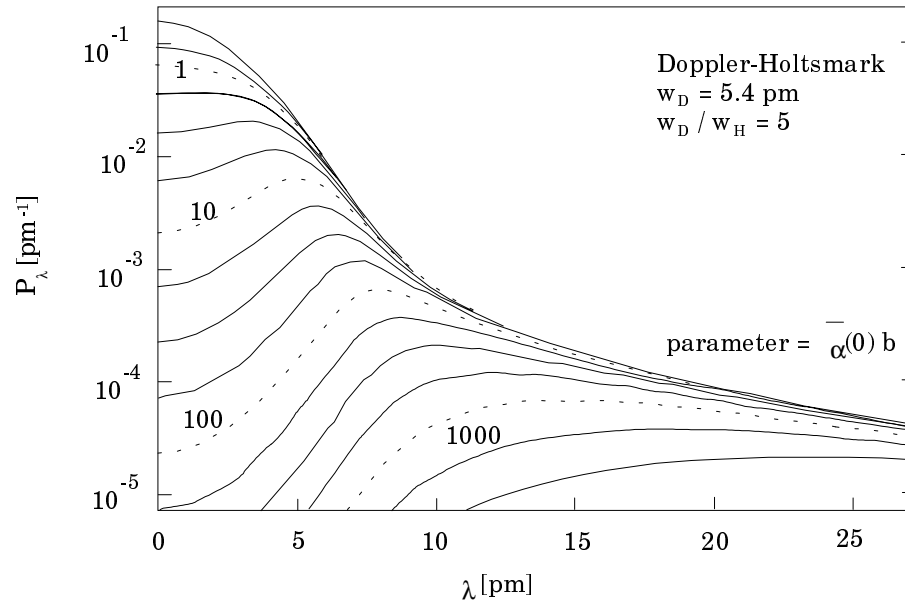


Fig. 3: Example for the calculation of spectral line profiles with various values of optical thickness. Shown is the convolution of a Doppler and a Holtzmark profile. The emission coefficient as a function of the plasma radius has a parabolic shape (case e3).

After integration of the spectral line profiles, the line escape factor is readily worked out. Examples for Doppler and Lorentz profiles, and for the three cases (e1) - (e3) are shown in Fig. 4. When the Lorentz profile is chosen, the calculation must be extended far into the line wings, because of their slow fall-off with wavelength. Figure 4 was calculated over 100 full half-widths to one side. The emitted radiation is highest for a constant spatial emission coefficient. If the emission is lower at the plasma edge, as in the cases (e2) and (e3), less optically thick radiation is emitted from the surface of the plasma and the corresponding escape factor is smaller. Linear and parabolic profiles behave very similarly here.

The results for the line escape factor and, as will be shown further down, also for the population escape factor apparently depend very critically on the spectral line profiles used and therefore, the profile shape must be an accessible input parameter for a general version of the program. It should be noted that in the present version of the main routine, the half-widths are assumed to be proportional to the centre wavelengths of the lines, as is the case for Doppler broadening.

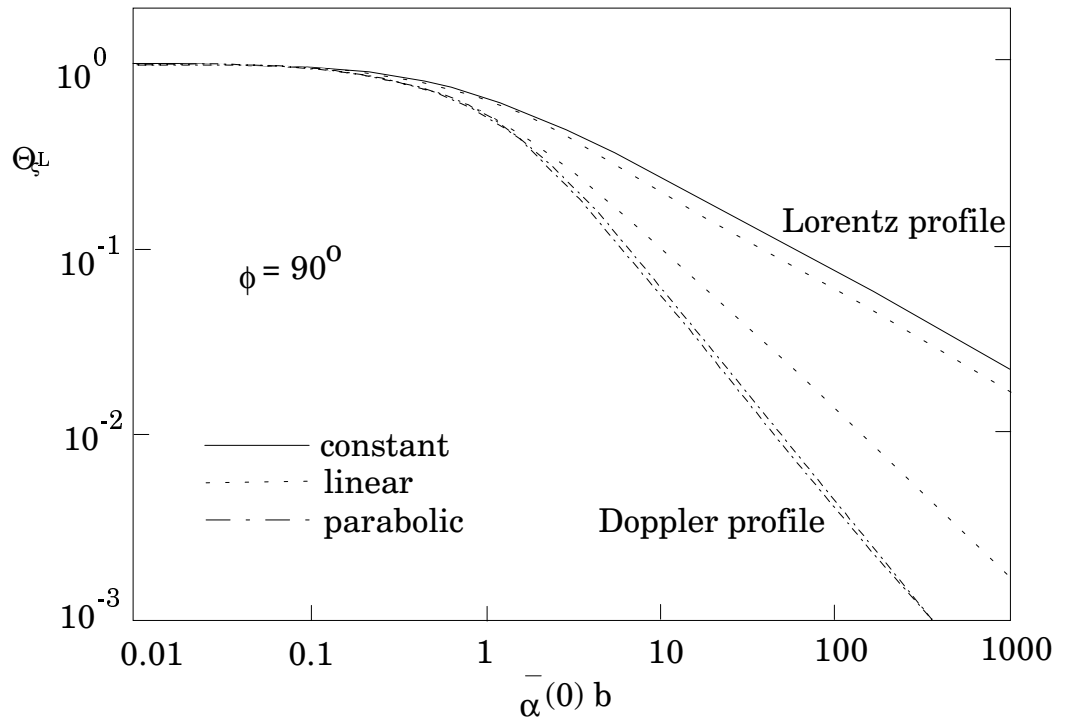


Fig. 4: Escape factors for perpendicular line emission. The influence of Doppler or Lorentz profiles is demonstrated, as well as the consequences for the spatial emission profiles (cases e1, e2 and e3).

Models for the Plasma Geometry

Again, three options are available for the plasma geometry, namely, (g1) an isotropic sphere with radius b (this does not require any additional calculation, since the solid angle integral is just 4π), (g2) a plane-parallel disk of thickness $2b$ and a diameter $2a$ and (g3), a cylinder with radius b and a length $2a$. The parameter a is specified by the 'aspect ratio' a/b in the code.

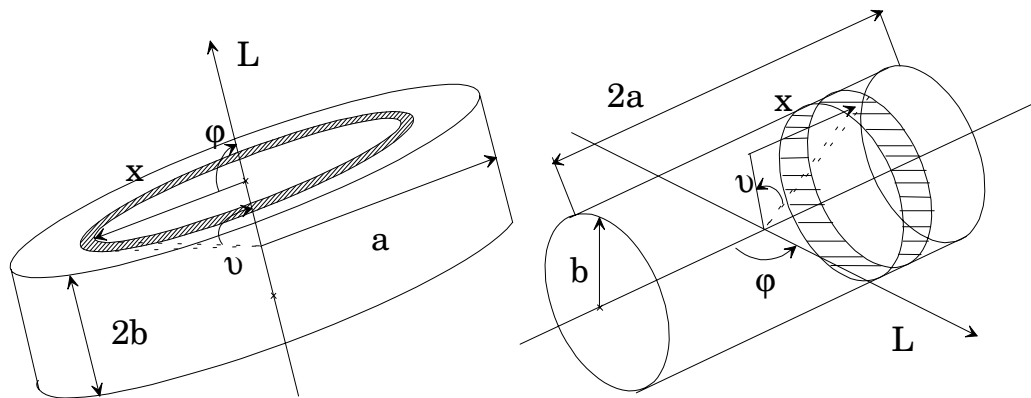


Fig. 5: Geometry for cases (g2), disk or slab, and (g3), cylinder. Explanation of the integration over solid angle for calculating the population escape factor. The spatial profiles of the emission coefficient, as well as the line escape factor apply to the direction of b .

The two latter geometrical models are shown in Fig. 5. Without further modification, the line escape factors described above immediately apply to the radiation emitted radially from the cylinder or perpendicular to the disk surface. For any other direction, the length must only be increased by $1/\sin\phi$, as defined in Fig. 5. This does not warrant an extra input parameter. The population escape factors for the isotropic case (sphere) and various line and spatial emission profiles are shown in Fig. 6. In this case, the absorption of light in the centre originating from

outer plasma zones is highest in the constant emission case, and therefore this population escape factor is at the lower side of the range.

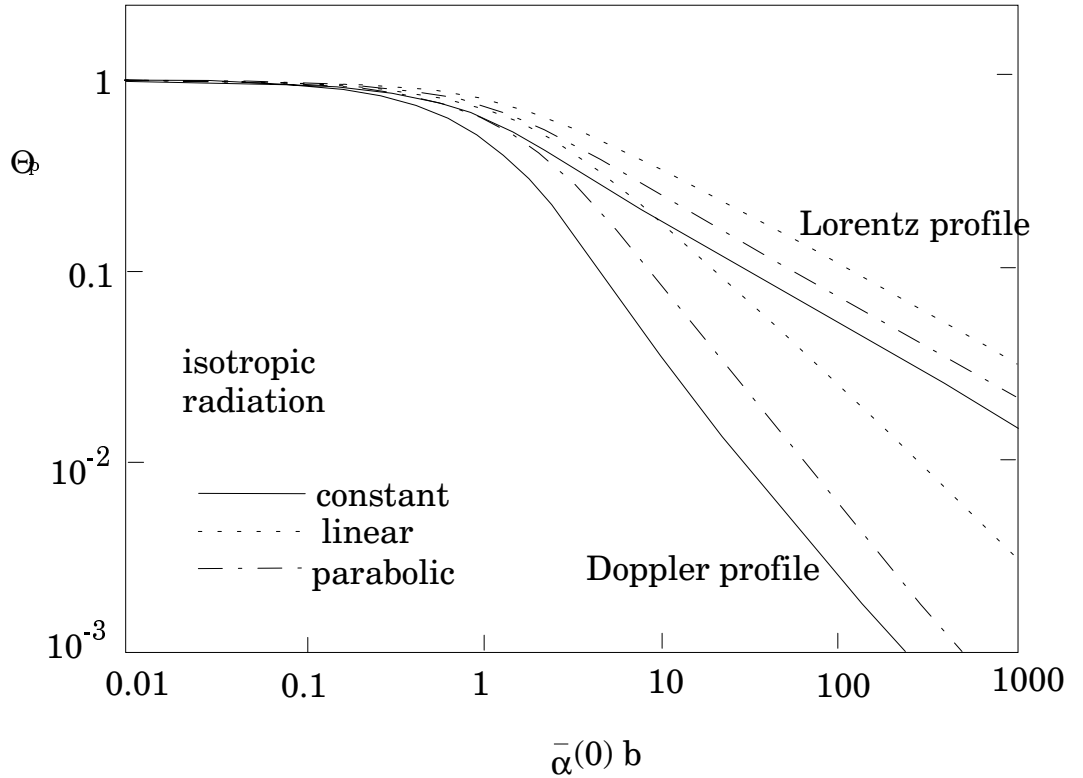


Fig. 6: Escape factors for population calculations. Isotropic (sphere, $g1$). The influence of Doppler or Lorentz profiles is demonstrated, as well as the consequences of the spatial emission profiles (cases $e1$, $e2$ and $e3$).

The integration over the solid angle in the plasma is done numerically in the program according to the scheme indicated in Fig. 5. The angle ϑ is used as variable and x calculated accordingly. The element $d\Omega$ follows from the projected area and the distance to the centre point, which also determines the length in the radiation transport equation. Care has been taken to arrive at precisely 4π after the Ω integration. Therefore, a correction has been implemented to account for the rim of the disk and the end planes of the cylinder by using appropriate average values. With these corrections, even cases with $a/b = 1$ can be treated with sufficient accuracy. Of course, once the optical depth is substantial, the results become independent of a , since the absorbed radiation comes from the immediate neighbourhood of the plasma centre.

The code extends both the population and line emission escape factors to greater optical depths by linearly extrapolating both these graphs.

Modification of ADAS adf04 Data Sets for Collisional-Radiative Model Calculations

The population escape factors, obtained in the described way, have always been used to modify transition probabilities in ADAS *adf04* data sets for subsequent collisional-radiative population calculations including opacity effects. For this purpose, the escape factor program first reads in the parameters for the normalised escape factor calculations, i.e. spectral line profile and plasma geometry information. Next, the program opens the *adf04* file defined in the input options widget. From the energy levels in this file it calculates the transition wavelengths and from the A -values and statistical weights the integrated absorption coefficients for density one. In order to derive the relevant lower state population from the provided total density of the species, the program must know the population of excited states including metastable levels. It is obtained by using a Boltzmann distribution according to the input electron temperature, T_e , and separate underpopulation factors for metastables and other levels. The actual ground state density is calculated by re-normalising the total population. As a further parameter, the spectral profile height in the line centre is required, which is derived from the normalised value of

$P_\lambda(0)$ and a width corresponding to the Doppler width for the input gas temperature and species mass. If a Doppler profile is chosen, the width is calculated from the input gas temperature and species mass. If Lorentzian or Holtsmark are chosen, the width is defined to be 0.5 of the Doppler width. For the convolution profiles (double Doppler, Voigt and Doppler-Holtsmark), one of widths is defined to Doppler, and the other is a factor of the Doppler width, the factor being entered by the user via a pop-up box when these profiles are selected. Together with the length parameter b from the input file, the relevant product $\bar{\alpha}(0)b$ for each transition is now worked out and the population escape factor obtained by a quadratic, logarithmic interpolation of the normalised results. The A-values in the adf04 file are modified accordingly and replaced in the respective line, and the data are written to the defined output data set with an appended comment giving the details of the relevant parameters of the run. If a transition is of an optical depth that is too great for its escape factor to be calculated, then its A-value is set to zero in the modified adf04 file, and a corresponding comment added to the file.

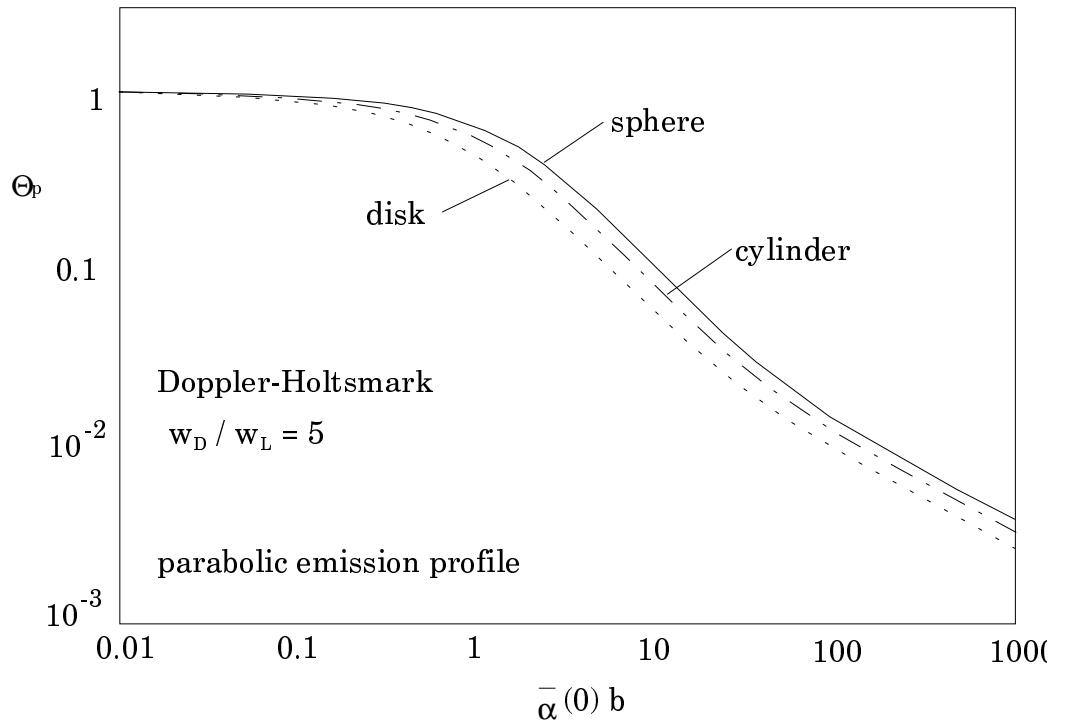


Fig. 7: Population escape factors for the three geometrical plasma models (g1) sphere, (g2) disk, and (g3) cylinder. The convolution of a Doppler and a Holtsmark profile is being used and the emission case is parabolic (e3).

The user is then free to process this modified adf04 file using ADAS205 or ADAS208 to calculate the opacity modified population distribution. If the code is enabled to run for a range of column densities then the modified *adf04* file is used to calculate the population distribution of all the levels via a statistical balance code, which is basically ADAS205. These modified populations are then re-entered into the escape factor code to calculate the line-of-sight escape factors along b , defined in fig 5, for each transition and this value used as a multiplier on the A-values. The modified A values along with the relevant upper level population densities are then used to calculate the ratio of emergent fluxes for selected transitions. The transitions to be considered are selected in the processing options screen and the ratios are shown for each transition relative to the first one selected.

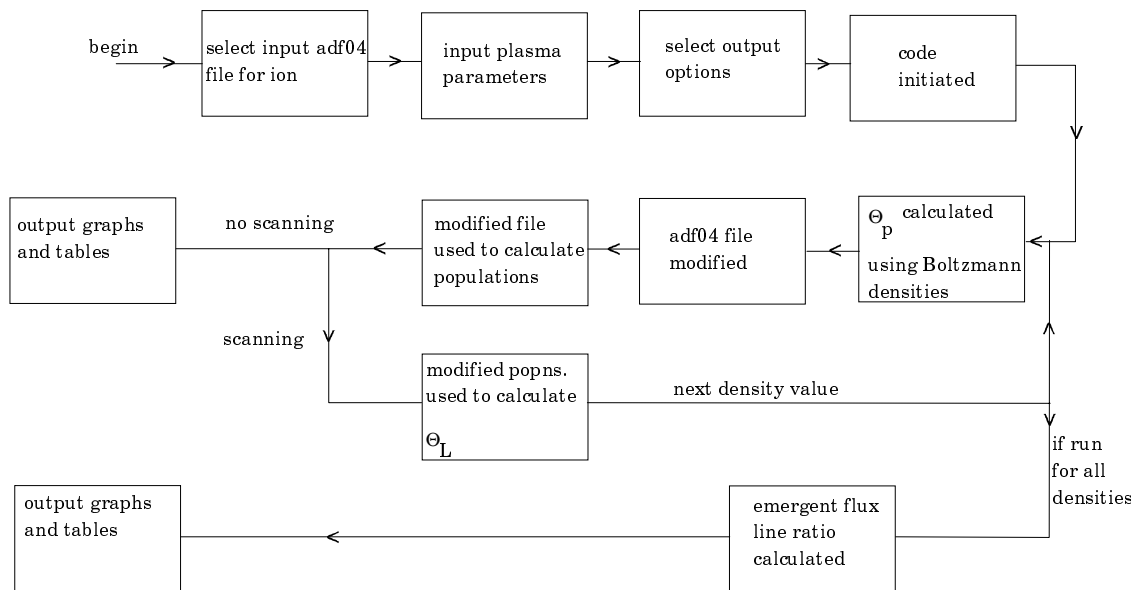
The code has three graphical and two text outputs. The code can either be run for one value of column density or for a range of column densities. If it is run for only one value, then the possible graphs are either the normalised escape factor vs. optical depth, or a graph of the line profile with modified profiles for a range of optical depths over-plotted. The textual output is

the *adf04* file, modified for the population escape factors, and the *paper.txt* file with the data from the two graphs described previously. If the code is run for a range of column densities, then the possible graphs are again the normalised escape factor vs optical depth, and one of the line profile with modified lines over-plotted (for the central column density chosen). The third graph is of the emergent flux ratio vs. column density for the selected transitions, each ratio being with respect to the first transition chosen in the processing options screen. The textual outputs are the *adf04* file modified for the population escape factor for the central column density chosen, and a *paper.txt* file with data from all three graphs.

Program steps:

These are summarised in figure 3.14.

Figure 3.14

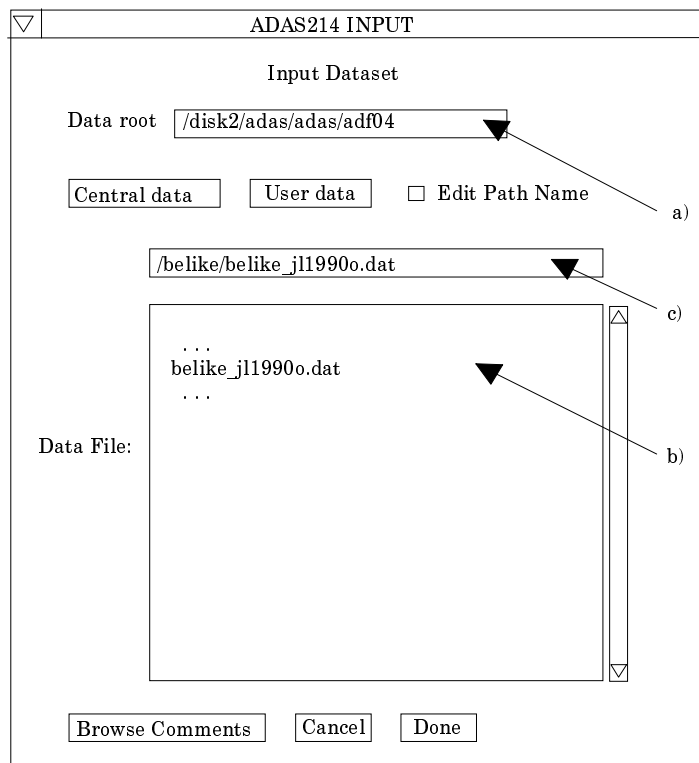


Interactive parameter comments:

Move to the directory in which you wish the standard ADAS created files to appear. For ADAS214, these are the output text file (*paper.txt*), and *adas214.pass*, the modified *adf04* file. The graphical output from the code are as described previously. Initiate ADAS214 from the program selection menus in the usual manner.

The **file selection window** appears first as illustrated below.

1. ADAS214 may access many data-sets during its operation. Buttons are present at a) to set the data root to that of the *Central data* or to your personal *User data* (provided it is in ADAS organisation). Alternatively, the data root may be edited explicitly
2. At b) identify and select the relevant *adf04* file for the ion in question.
3. c) displays the *adf04* file that has been selected from the relevant directory.
4. Clicking the *Done* button moves you forward to the next window. Clicking the *Cancel* button takes you back to the previous Series 2 menu. Clicking the browse button brings up any existing comments on the selected *adf04* file.



The **processing options window** is shown below.

5. A summary of the *adf04* data file selected is given at a).
6. The selection of temperatures, densities and other plasma parameters are made at b). The following parameters need to be entered: atomic mass number, electron temperature (this is only used to calculate the Boltzmann density distribution), gas temperature, density, length of plasma (b in fig 5), aspect ratio (a/b in fig 5), line profile, density distribution across plasma and plasma geometry.
7. The table to select the transitions to be observed for their variation in emergent flux ratios the may be edited by clicking on the *Edit Table* button. The ADAS Table Editor is then presented with the usual set of editing operations available. The normalised escape factor plot will show the predicted optical depths for the transitions chosen here. If scanning is enabled, then emergent flux line ratios can be plotted for each transition with respect to the first one selected in the table.
8. In the metastable and Boltzmann deviation window, c), one can enter at d) a factor to alter the Boltzmann density of the respective levels. If no multiplier is entered, the level is assumed to be under-populated to 1/10th of its Boltzmann value. This is only used to get an initial estimate of the populations, to be used to calculate the population escape factors.
9. If scanning is not selected, the code is run for the values selected. If scanning is selected, then the code is run for a range of column densities, the range being given by the maximum and minimum factors entered below the scanning button for the number of steps chosen.
10. Clicking the *Done* button causes the next output options window to be displayed. *Cancel* takes you back to the previous window and the *Escape to Menu* icon is also available for a quick exit at the bottom left hand corner.

ADAS209 : PROCESSING OPTIONS

Data File Name :
/disk2/adas/adas/adf04/belike/belike_j11990o.dat

Browse Comments

Atomic Mass Number

Select Line Profile
 Doppler
 Lorentzian
 Holtzmark
 Double Doppler
 Voigt
 Doppler Holtz.

Select Density Dist.
 Homogeneous
 Linear
 Parabolic

Select Plasma Geom.
 Sphere
 Disk
 Cylinder

Scan ? Yes No
 No. of steps
 Min. factor Max. factor

Density (cm⁻³)
 Dimension (b) (cm)

Ion Temp (K)
 Boltz. E-Temp (K)
 Aspect ratio (a/b)

Observed Spectrum Lines
 Index Upper Lower
 level level

Edit Table

Designate metastables and Boltzmann Deviations

Enter a multiplier for each metastable
 < Press return after each entry >

1	2s2(1s0)	(1)0(0.0)	0.0	1	
2	2s2p(3P0)	(3)1(0.0)	81942.5	2	
3	2s2p(3P1)	(3)1(1.0)	82078.6	2	
4	2s2p(3P2)	(3)1(2.0)	82385.3	2	
	...				
	...				
	...				
	...				
	...				
	...				
	...				

Cancel Done

The **output options window** is shown below.

11. Information is again given of the input *adf04* file at a).
12. The *graphical output* button at b) must be selected to enable the generation of graphs. The graph title is also entered at b).
13. If the *explicit scaling* button is selected, the plotting range can be forced manually, the ranges being entered in the boxes provided. If scaling isn't selected, the program finds the most relevant range itself to plot the chosen graph.
14. The output graph to be generated is selected in the box to the right of the explicit scaling box. Graph 1 is the Normalised escape factor vs. Optical depth curve. Graph two is of the line profile and graph 3 is the emergent flux intensity ratio as a function of column density for the selected transitions and is only available if the scanning option is selected.
15. The *hard copy* button enables the generated graph to be sent to file for printing. The filename is entered in the box provided, and the printer device selected from the list. It is to be noted that the *print* button on the graph window will still have to be pressed for the graph to be sent to file.
16. The usual text output file summarising the processing may be produced. Make the required selections at d).
17. The modified *adf04* file can be written to file by making the required selection at e)
18. Clicking the *Done* button causes the calculation to commence. Clicking the *Cancel* button takes the user back to the previous window and clicking the *Escape to Menu* button returns to the ADAS menu screen

Illustration:

Example (1) - Carbon III lines in the solar atmosphere

The first example given is based on a study of CIII spectral line ratios in the solar atmosphere [9]. The multiplet under investigation is CIII $2s2p^3P - 2p2^3P$ (1175A), with two line ratios to be considered. The first ratio, the 0-1/2-1 (where numbers here are the J quantum numbers of the levels, with the first number being the lower level) was expected to be insensitive to opacity, whilst the other ratio, 2-2/1-2, was expected to show opacity effects. The lines were measured using the SUMER instrument on the SOHO satellite, and involved 18 raster position observations, crossing the limb of the Sun. It was expected that at the limb, the geometrical thickening of the line of sight would lead to increased opacities in the sensitive lines. In the observations, the sensitive ratio started at approximately three on disk and decreased to about one at the limb.

The plasma under consideration was the solar atmosphere, from just below the limb, to significantly beyond the limb. Thus the expected plasma parameters were, density = $5 \times 10^{10} \text{ cm}^{-3}$, electron temperature = 80,000K, ion temperature = 80,000K. The line widths were expected to be dominated by Doppler broadening, and the density was assumed to be homogenous throughout the layer in question. For this application it is assumed that only the ground and the metastable state have their Boltzmann population densities, with the rest being under-populated. The geometry was assumed to be Disk, with length 1000cm and aspect ratio 10000. With the aspect ratio chosen to be such a large value, the geometry approximates to a large slab, and is close to the plane parallel geometry assumed in the solar atmosphere.

Upon starting ADS214, the first thing to be selected is the *adf04* file. Looking in the standard ADAS *adf04* file library, under directory *copjl#be* ions, the following data set was found *copjl#be_jl#c2j.dat*.

It was found useful to first find if the lines chosen were optically thick for the column density chosen. Thus, scanning was disabled. The Normalised escape factor profile was chosen giving

the graph of figure 3.14a. As can be seen, the two lines in question, have different optical thicknesses, while the insensitive lines have similar opacities and will vary by similar amounts as the column density of the plasma increases. This step is useful for getting a first estimate of the effects of opacity on the lines you have chosen.

Figure 9 - Normalised escape factor for CIII

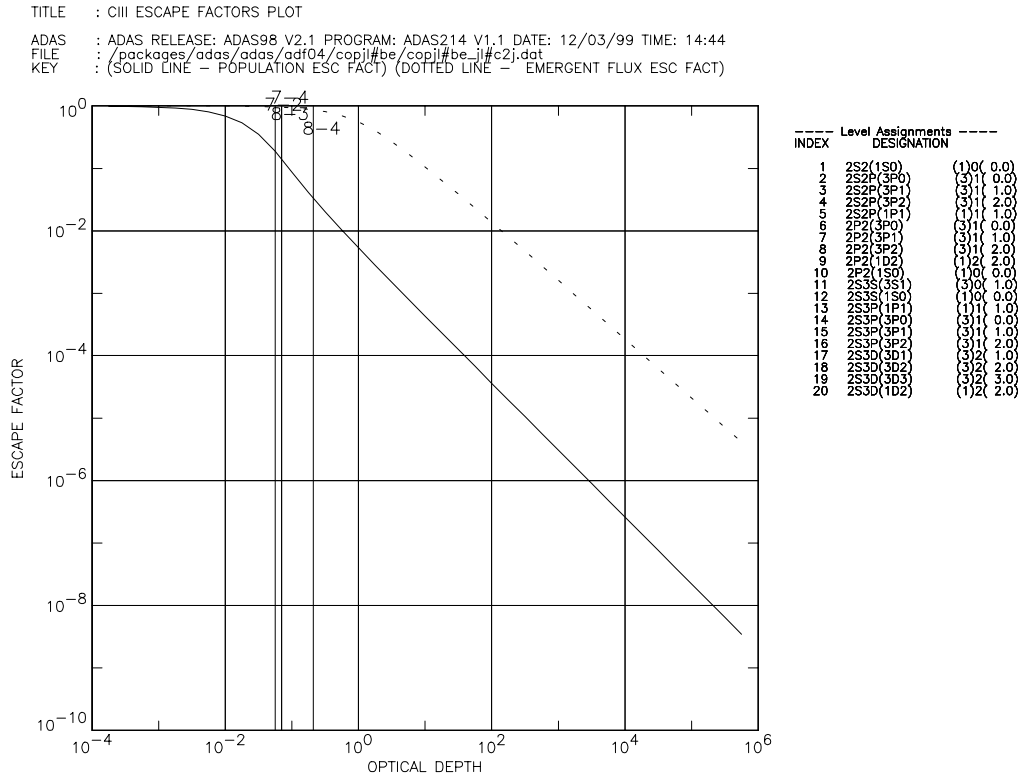


Table 3.14a Escape factor modified ADF04 file

```

C + 3      6      3      386241.
1  2S2(1S0)      (1)0( 0.0)      0.0
2  2S2P(3P0)     (3)1( 0.0)     52367.1
3  2S2P(3P1)     (3)1( 1.0)     52390.8
4  2S2P(3P2)     (3)1( 2.0)     52447.1
5  2S2P(1P1)     (1)1( 1.0)     102352.0
6  2P2(3P0)      (3)1( 0.0)     137425.7
7  2P2(3P1)      (3)1( 1.0)     137454.4
8  2P2(3P2)      (3)1( 2.0)     137502.0
9  2P2(1D2)      (1)2( 2.0)     145876.1
10 2P2(1S0)      (1)0( 0.0)     182519.9
11 2S3S(3S1)     (3)0( 1.0)     238213.0
12 2S3S(1S0)     (1)0( 0.0)     247170.3
13 2S3P(1P1)     (1)1( 1.0)     258931.3
14 2S3P(3P0)     (3)1( 0.0)     259705.6
15 2S3P(3P1)     (3)1( 1.0)     259711.2
16 2S3P(3P2)     (3)1( 2.0)     259724.3
17 2S3D(3D1)     (3)2( 1.0)     270010.8
18 2S3D(3D2)     (3)2( 2.0)     270011.9
19 2S3D(3D3)     (3)2( 3.0)     270014.7
20 2S3D(1D2)     (1)2( 2.0)     276482.9
-1
3.00      3      9.00+03  1.80+04  4.50+04  9.00+04  1.80+05  4.50+05  9.00+05  1.80+06
2  1  1.00-30  1.19-01  1.13-01  1.08-01  9.51-02  7.81-02  5.44-02  3.84-02  2.44-02
3  1  1.04+02  3.58-01  3.40-01  3.23-01  2.85-01  2.34-01  1.63-01  1.15-01  7.32-02
4  1  5.22-03  5.96-01  5.67-01  5.39-01  4.75-01  3.91-01  2.72-01  1.92-01  1.22-01
5  1  3.47+07  3.75+00  3.88+00  4.10+00  4.48+00  5.15+00  6.64+00  8.07+00  9.93+00
6  1  1.00-30  1.30-03  1.75-03  2.47-03  2.53-03  2.17-03  1.46-03  9.75-04  7.55-04
7  1  9.23-04  3.89-03  5.25-03  7.41-03  7.60-03  6.50-03  4.38-03  2.93-03  2.27-03
8  1  3.83-02  6.48-03  8.75-03  1.24-02  1.27-02  1.08-02  7.31-03  4.88-03  3.78-03
. . .
19 16 6.99+06  4.36+01  4.82+01  6.36+01  8.35+01  1.07+02  1.42+02  1.72+02  2.03+02
20 16 1.00-30  1.55+00  1.44+00  1.26+00  1.07+00  8.30-01  4.96-01  3.01-01  1.75-01
20 17 1.00-30  1.83+00  1.69+00  1.46+00  1.22+00  9.35-01  5.63-01  3.49-01  2.03-01
20 18 1.00-30  3.04+00  2.82+00  2.43+00  2.04+00  1.56+00  9.38-01  5.81-01  3.39-01

```

```

20 19 1.00-30 4.26+00 3.94+00 3.40+00 2.85+00 2.18+00 1.31+00 8.13-01 4.74-01
-1
-1 -1
C-----
C
C      . . .
C      J LANG      June 1995.
C-----
C-----
c 12/03/99
c produced with ADAS214 and the following data:
c input data file: /packages/adas/adas/adf04/copjl#be/copjl#be_jl#c2j.dat
c dens distn: Homogeneous
c geometry: Disk
c profile: Doppler
c m = 1., Te = 80000.0K, Tg = 80000.0K, l = *****cm,
c na or nion = 5.00D+10cm-3
C-----

```

Because we do not know the plasma density and length very accurately, it was decided to run the code for a wide range of column densities. Thus, the minimum factor was set to 0.1 and the maximum factor set to 100. The number of steps was set to 10. This time we select the ratio plot graph generating figure 3.14b below.

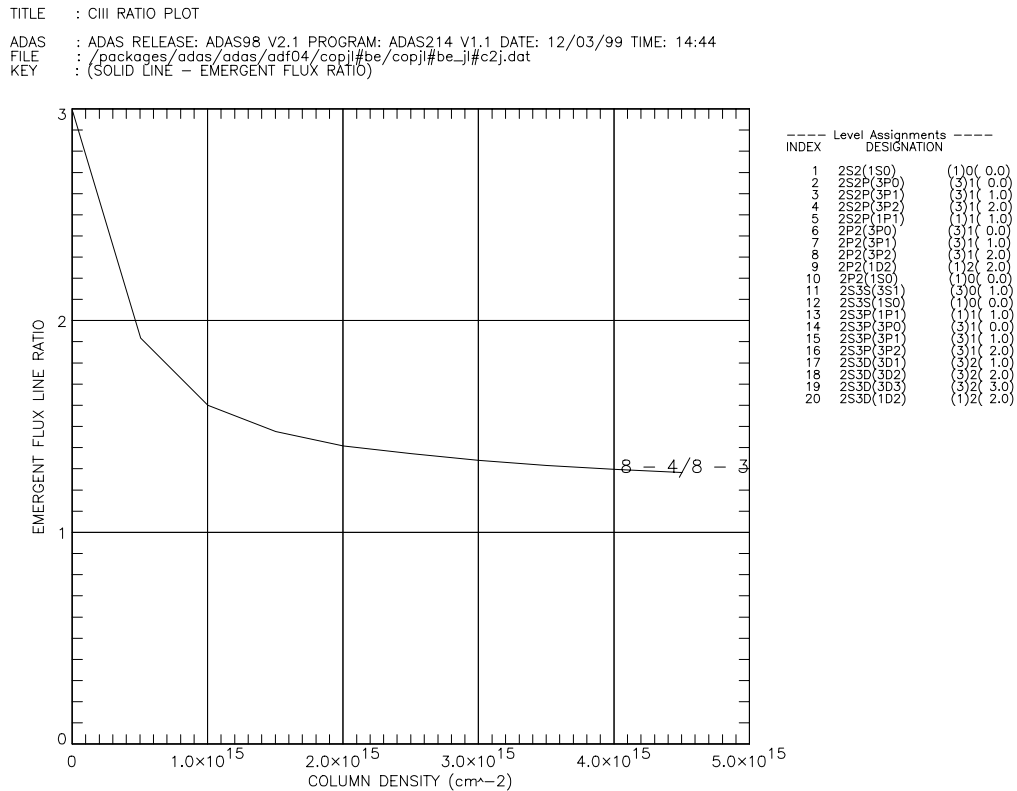
As can be seen from the figure 3.14b, the results from the ADAS code is consistent with the observed ratios. This compares well with expected results implied from Brooks et. al.(1998).

Example (2) - Hydrogen, investigating H-alpha and H-Beta

The second example given corresponds to a study by Behringer [8] on neutral density measurements in the ASDEX divertor. In ASDEX Upgrade discharges approaching the density limit, the divertor plasmas near the target plates become cold and dense, the flows stagnate and the electrons and ions start to recombine effectively in the plasma volume. This leads to substantial neutral densities in the divertor region. Under these conditions, the hydrogen Lyman lines become optically thick with all the consequences for ionisation balance and radiation. The only simple method for measuring the neutral hydrogen density in this region consists of analysing the absorption or self-absorption of the Lyman resonance lines.

In the experiment performed, the Hydrogen lines H α and L β (branching ratio transitions) were measured simultaneously during the density ramp up. It was observed that with increasing density, the ratio of the two lines in the inner divertor changed by about a factor of four between low densities and density = 10^{14} cm^{-3} , which can only be due to the optical thickness of L β . ADAS214 can be used to calculate an approximate value for the neutral density from these results.

Figure 10 - Ratio plot for CIII



The spectral line profile of $L\beta$ is determined by Doppler broadening with several possible contributions, but also by Zeeman splitting and by the linear Stark effect. From an investigation into the broadening mechanisms of this line (see Gunter [6] and Behringer[10]), a convolution of a Doppler profile of width 7pm and a Lorentz profile of width 1pm was chosen. The spectral line profile does not, in this case represent a major source of uncertainty in the calculation. To implement this in the processing option window, the Voigt profile was chosen, with the factor on the second width entered as 0.14. The effective length of the plasma was calculated (see [7] and [8]) to be 7.5cm, and the density profile assumed to be parabolic with an input density of 1.0^{14} cm^{-3} . The input *adf04* file was chosen to be *copha#h_bn#97h.dat*. The first level was assumed to be at its Boltzmann value, the rest assumed to be under-populated. The transitions chosen in the table were 3-2 and 3-1, corresponding to H-alpha and L-beta. The plasma geometry was chosen as cylindrical. The gas temperature was chosen to be 23010K and the electron temperature 11605K, finally the aspect ratio was entered as 5.

The code can be run for no scanning, and the normalised escape factor plot chosen. Figure 3.14c shows the expected optical depths for each of the lines under investigation. As can be seen, the L-beta line is expected to be optically thick for the parameters chosen. Scanning is selected, with minimum factor set to 0.8 and maximum factor set to 2.0, and the graph of figure 3.14d generated. From the print out of the graph result, in the *paper.txt* file, a ratio of four corresponds to a density of $1 \times 10^{20} \text{ m}^{-3}$. This result is very much consistent with divertor code calculations.

Figure 11 - Normalised escape factor for H

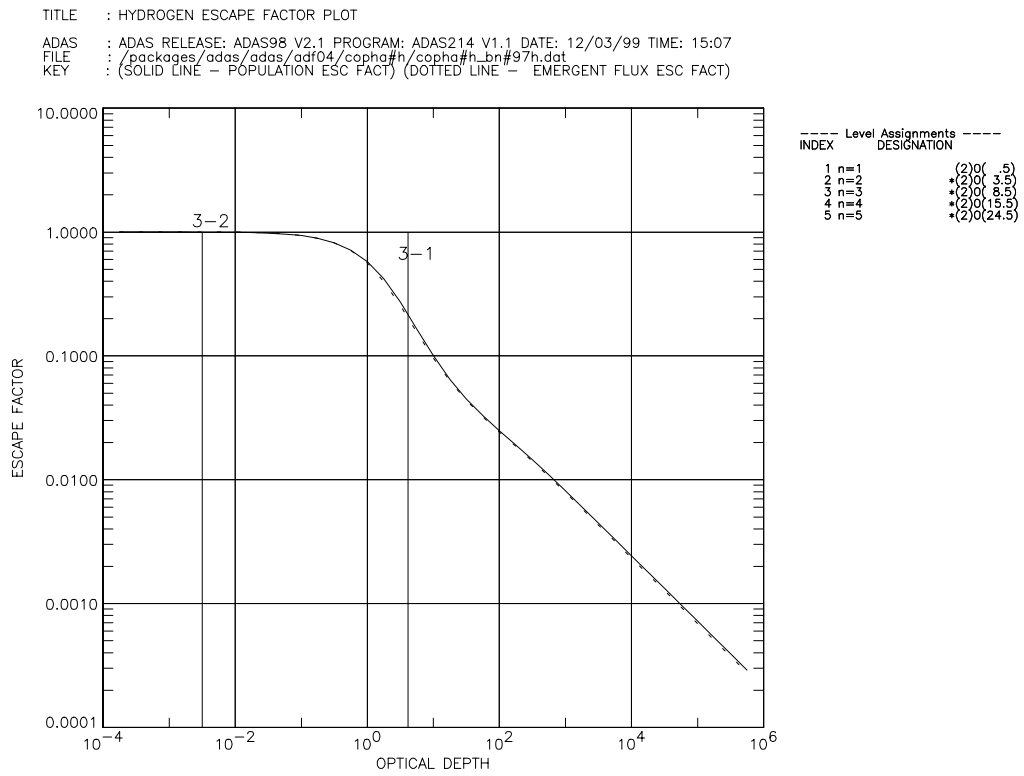


Figure 12 - Ratio plot for H

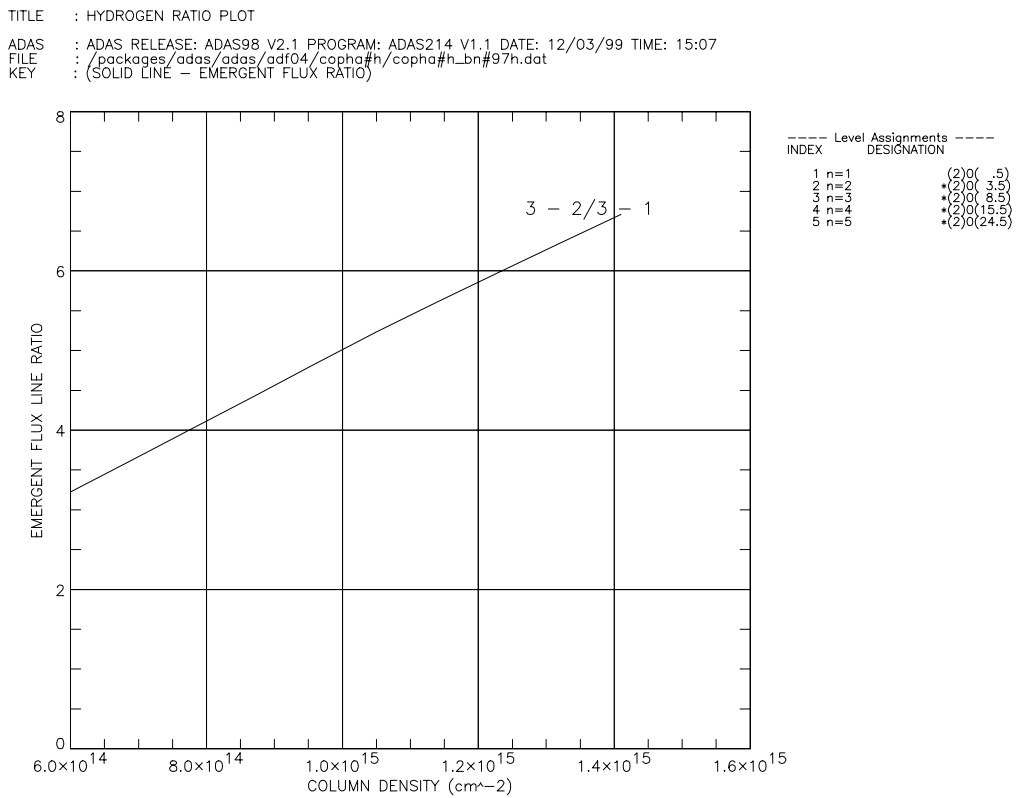


Table 3.14b Standard text output showing line ratio calculation

```

ADAS RELEASE: ADAS98 V2.1 PROGRAM: ADAS214 V1.1 DATE: 12/03/99 TIME: 15:07
***** TABULAR OUTPUT FROM ESCAPE FACTORS PROGRAM: ADAS214 - DATE: 12/03/99 *****
H + 0      1      1      109679.0(1S)
  1 n=1      (2)0( .5)      .0 {1}1.000
  2 n=2      *(2)0( 3.5)      82259.0 {1}1.000
  3 n=3      *(2)0( 8.5)      97492.0 {1}1.000
  4 n=4      *(2)0(15.5)     102824.0 {1}1.000
  5 n=5      *(2)0(24.5)     105292.0 {1}1.000
-1
-----
C
Optical Depth      Population Escape Factor
0.178E-03      0.100E+01
      . . .
      . . .
0.562E+06      0.290E-03
-----
C
Optical Depth      Emergent Flux Escape Factor
0.178E-03      0.100E+01
      . . .
      . . .
0.562E+06      0.276E-03
-----
C
Profile Intensity      Wavelength(from line centre) /pm
0.750E-01      0.108E+01
      . . .
      . . .
0.315E-06      0.866E+03
-----
C
Transition      Column Density
Upper Lower      (CM-2)= 6.0000E+14 6.9000E+14 7.8000E+14 8.7000E+14 9.6000E+14 1.0500E+15
1.1400E+15 1.2300E+15 1.3200E+15 1.4100E+15 1.5000E+15
      3      1      1.0000E+00 1.0000E+00 1.0000E+00 1.0000E+00 1.0000E+00 1.0000E+00 1.0000E+00
1.0000E+00 1.0000E+00 1.0000E+00 1.0000E+00 0.0000E+00
      3      2      3.2241E+00 3.6236E+00 4.0247E+00 4.4278E+00 4.8333E+00 5.2325E+00
5.6102E+00 5.9820E+00 6.3481E+00 6.7090E+00 0.0000E+00
-----
C
c 12/03/99
c produced with ADAS214 and the following data:
c input data file: /packages/adas/adas/adf04/copha#h/copha#h_bn#97h.dat
c dens distn.: Parabolic
c geometry: Cylinder
c profile: Voigt
c m = 1., Te = 11605.0K, Tg = 23010.0K, l = 7.50cm,
c na or nion = 1.40D+14cm-3
-----

```

References:

- [1] F.E. Irons, The Escape Factor in Plasma Spectroscopy - I. The Escape Factor Defined and Evaluated, JQSRT 22, 1 (1979)
- [2] SFB 259, Bericht über Hochtemperaturprobleme ruckkehrfähiger Raumtransportsysteme, Arbeits- u. Ergebnisbericht, Universität Stuttgart, 1992
- [3] H. Jentschke, Spektroskopische Untersuchung eines luftähnlichen Plasmastreifens, Thesis, Institut für Plasmaforschung, Universität Stuttgart, 1995
- [4] K. Behringer, The Influence of Opacity on Hydrogen Line Emission and Ionisation Balance in High Density Divertor Plasmas, Max-Planck-Institute for Plasma Physics Report, IPP 10/5 (1997)

- [5] H.P. Summers, L. Wood, Ionisation, Recombination and Radiation of Impurities in Plasmas, JET Report, JET Joint Undertaking Report R(88)06 (1988).
- [6] S. Gunter, private communication, IPP 1998
- [7] R. Schneider, private communication, IPP 1998
- [8] U. Wenzel et al., Plasma Parameters and Volume Recombination in the ASDEX Upgrade Divertor I, to be published 1998
- [9] Brooks et. al., submitted, 1998
- [10] K.Behringer, Escape Factors for Line Emission and Population Calculations, Max-Planck-Institute for Plasma Physics Report, IPP 10/11 (1998).

Notes